

1
2
3
4
5
6
7
8
9
10
11
12
13
14
15
16
17
18
19
20
21
22
23
24
25
26
27
28
29
30
31
32
33
34
35
36
37
38
39
40
41
42
43
44
45
46
47
48
49
50
51
52
53
54
55
56
57
58
59
60
61
62
63
64
65

1 Commonalities of carbon dioxide exchange in semiarid regions with monsoon and
2 Mediterranean climates

3
4 Russell L. Scott¹, Penélope Serrano-Ortiz^{2, 3}, Francisco Domingo², Erik P. Hamerlynck¹, Andrew S.
5 Kowalski^{3, 4}

6
7 ¹USDA-ARS Southwest Watershed Research Center, Tucson, AZ USA

8 ²Estación Experimental de Zonas Áridas, Consejo Superior de Investigaciones Científicas,
9 Almería, Spain

10 ³Centro Andaluz de Medio Ambiente, Granada, Spain.

11 ⁴Departamento de Física Aplicada, Universidad de Granada, Granada, Spain.

12
13
14
15
16
17
18
19
20 Corresponding author:

21 Russell L. Scott, Ph.D.
22 Southwest Watershed Research Center
23 USDA-ARS
24 2000 E. Allen Road
25 Tucson, AZ 85719
26 USA
27
28 russ.scott@ars.usda.gov
29 phone: 01.520.647.2971
30 fax: 01.520.670.5550
31

1
2
3
4
5
6
7
8
9
10
11
12
13
14
15
16
17
18
19
20
21
22
23
24
25
26
27
28
29
30
31
32
33
34
35
36
37
38
39
40
41
42
43
44
45
46
47
48
49
50
51
52
53
54
55
56
57
58
59
60
61
62
63
64
65

32 Abstract

33 Comparing biosphere-atmosphere carbon exchange across monsoon (warm-season rainfall)
34 and Mediterranean (cool-season rainfall) regimes can yield information about the interaction
35 between energy and water limitation. Using data collected from eddy covariance towers over
36 grass and shrub ecosystems in Arizona, USA and Almeria, Spain, we used net ecosystem carbon
37 dioxide exchange (NEE), gross ecosystem production (GEP), and other meteorological variables
38 to examine the effects of the different precipitation seasonality. Considerable crossover
39 behavior occurred between the two rainfall regimes. As expected in these usually water-limited
40 ecosystems, precipitation magnitude and timing were the dominant drivers of carbon
41 exchange, but temperature and/or light also played an important role in regulating GEP and
42 NEE at all sites. If significant rainfall occurred in the winter at the Arizona sites, their behavior
43 was characteristically Mediterranean whereby the carbon flux responses were delayed till
44 springtime. Likewise, the Spanish Mediterranean sites showed immediate pulse-like responses
45 to rainfall events in non-winter periods. The observed site differences were likely due to
46 differences in vegetation, soils, and climatology. Together, these results support a more unified
47 conceptual model for which processes governing carbon cycling in semiarid ecosystems need
48 not differ between warm-season and cool-season rainfall regimes.

50 Keywords: semiarid, carbon dioxide, Mediterranean, monsoon, net ecosystem exchange

1
2
3
4
5
6
7
8
9
10
11
12
13
14
15
16
17
18
19
20
21
22
23
24
25
26
27
28
29
30
31
32
33
34
35
36
37
38
39
40
41
42
43
44
45
46
47
48
49
50
51
52
53
54
55
56
57
58
59
60
61
62
63
64
65

51 Introduction

52 Arid and semiarid areas occupy around one third of the Earth's land surface (Schlesinger et al.,
53 1990) and store about 15% of the world's surface organic carbon (Lal, 2004) and 20-30% of the
54 total organic and inorganic carbon (Eswaran et al., 2000; Rasmussen, 2006). In these dryland
55 regions, water is the major limiting element for ecosystem mass exchange and productivity
56 (Noy-Meir, 1973) as well as an important factor in how energy from net radiation is partitioned
57 at the land surface (Small and Kurc, 2003). As most of the world's ecosystems experience
58 substantial water limitation for some part of the year (Jenerette et al., 2011), studies of
59 aridland water and carbon exchange can give important and more broadly applicable insights
60 into water-limited ecosystem functioning.

61 Semiarid landscapes worldwide are under increasing pressures to provide products and services
62 to expanding human populations and economic activity. In these regions precipitation is often
63 sporadic and seasonal. Among semiarid zones, temperate monsoon and Mediterranean
64 climates represent important extremes of seasonal precipitation as monsoon systems have
65 concentrated rainfall in the warm, summer season, while in Mediterranean areas much of the
66 precipitation occurs in the cool season. These seasonal changes in atmospheric forcing via
67 inputs of radiation, temperature, vapor pressure, and wind provide an opportunity to see how
68 other constraints besides water limitation may play roles in governing ecosystem carbon
69 exchange.

70 In semiarid monsoon, or warm-season, precipitation systems, rainfall arrives around the peak in
71 atmospheric energy input. This brings about a strong competition for soil water between plants
72 and direct evaporation to the atmosphere from bare soil, demanding a fast response by the

1
2
3
4
5
6
7
8
9
10
11
12
13
14
15
16
17
18
19
20
21
22
23
24
25
26
27
28
29
30
31
32
33
34
35
36
37
38
39
40
41
42
43
44
45
46
47
48
49
50
51
52
53
54
55
56
57
58
59
60
61
62
63
64
65

73 vegetation to quickly use, or lose, available water. The sporadic nature of rainfall, as well as the
74 response of the ecosystem to it, gives rise to the Pulse paradigm (Huxman et al., 2004; Noy-
75 Meir, 1973; Reynolds et al., 2004). This paradigm for ecosystem CO₂ cycling posits that small
76 rainfall events provoke quick periods, or pulses, of heterotrophic respiratory efflux but do not
77 evoke a photosynthetic response (Huxman et al., 2004). Larger precipitation events (> ~10 – 20
78 mm) are needed to sufficiently moisten the soil to greater depths (> ~5 - 10 cm) to provoke
79 longer-term pulses of photosynthesis and autotrophic respiration due to plant growth. Total
80 seasonal rainfall is strongly correlated with the number of larger storms (Emmerich, 2007;
81 Huxman et al., 2004), and thus total photosynthesis is well correlated with seasonal rainfall
82 totals in these regions (Anderson-Teixeira et al., 2011; Kurc and Small, 2007; Scott et al., 2010;
83 Scott et al., 2009). Likewise, in above-average rainfall years these ecosystems tend to be sinks
84 of carbon (Anderson-Teixeira et al., 2011; Emmerich, 2003; Leuning et al., 2005; Mielnick et al.,
85 2005; Scott et al., 2010; Scott et al., 2009). Much less is known about constraints other than
86 water in semiarid monsoon systems that may occur outside the main growing season,
87 especially in mid-latitude regions where the seasonal shift in climate forcing is substantial.
88 In Mediterranean, or cool-season, precipitation climates, water arrives when the atmospheric
89 energy inputs are reduced and thus, water availability and available energy are strongly
90 asynchronous. When the energy is low, unlike the fast response to rain events for monsoonal
91 systems, water tends to accumulate in the soil until there is enough energy to activate
92 respiratory and photosynthetic responses. Photosynthesis and respiration fluxes peak in the
93 spring or early summer depending on precipitation season length, soil moisture storage,
94 temperature, and light. This biological activity then tapers off and ceases as the dry season

1
2
3
4 95 progresses and soil moisture becomes more limiting. Thus, in Mediterranean systems there
5
6
7 96 are strong correlations between total photosynthesis and winter and spring rainfall totals (Aires
8
9
10 97 et al., 2008; Ma et al., 2007) or even total annual precipitation (Xu and Baldocchi, 2004).
11
12 98 However, while there is a positive relationship between yearly precipitation and net ecosystem
13
14
15 99 exchange of CO₂ (NEE) (Luo et al., 2007), the variability in NEE is more strongly correlated with
16
17 100 the timing of the rainfall and winter temperatures that determine the growing season length
18
19
20 101 (Ma et al., 2007; Serrano-Ortiz et al., 2009). For some Mediterranean ecosystems, interpreting
21
22 102 net CO₂ exchanges during dry season conditions is further complicated by ventilation of CO₂
23
24
25 103 from carbonate-rich soil, which may or may not have a biological source (Rey et al., 2012;
26
27
28 104 Sanchez-Cañete et al., 2011; Serrano-Ortiz et al., 2009; Serrano-Ortiz et al., 2010).
29
30
31 105 In this paper we compare and contrast responses of two semiarid monsoon and two
32
33
34 106 Mediterranean ecosystems to examine how precipitation seasonality influences patterns of
35
36 107 ecosystem photosynthesis and net CO₂ flux. By doing so, we highlight when these fluxes are
37
38
39 108 limited by atmospheric conditions or surface water supply. Also, we ask if there were
40
41
42 109 crossovers in behavior that may blur the lines between monsoonal and Mediterranean
43
44 110 responses. For example, are there times when Mediterranean systems display rapid pulse-like
45
46
47 111 responses, and conversely, are there times when monsoon-dominated systems are constrained
48
49 112 by cooler winter-season temperatures? To address these questions, we test the following
50
51
52 113 hypotheses: 1) monsoon ecosystems given sufficient wintertime precipitation, exhibit a
53
54 114 “Mediterranean response” , whereby the response of photosynthesis and net CO₂ uptake are
55
56
57 115 delayed till spring, and 2) Mediterranean systems exhibit “monsoon” or pulse-like responses of
58
59 116 photosynthesis and NEE when significant precipitation (> ~ 10 mm) falls in the non-winter
60
61
62
63
64
65

1
2
3
4
5
6
7
8
9
10
11
12
13
14
15
16
17
18
19
20
21
22
23
24
25
26
27
28
29
30
31
32
33
34
35
36
37
38
39
40
41
42
43
44
45
46
47
48
49
50
51
52
53
54
55
56
57
58
59
60
61
62
63
64
65

117 season. Moreover, we ask whether seasonal precipitation has the same effect on ecosystem
118 photosynthesis and hypothesize that: 3) monsoon ecosystem photosynthesis is more responsive to
119 variations in precipitation than in Mediterranean systems due to the co-occurrence of precipitation and
120 warmer temperatures conducive to plant activity.

121 Methods

122 Meteorological and flux data collected for this study were collected over a grassland and
123 savanna in southern Arizona, USA and a grassland and shrubland in Almería, southern Spain.
124 Table 1 summarizes basic climate and vegetation information about the sites. At all sites, the
125 eddy covariance technique was used to measure land-atmosphere fluxes, and
126 micrometeorological measurement details for each site are presented elsewhere (Rey et al.,
127 2012; Scott et al., 2010; Scott et al., 2009; Serrano-Ortiz et al., 2009). In brief, the wind and
128 sonic temperature were sampled at 10 Hz by 3D sonic anemometers (CSAT3, Campbell
129 Scientific Inc., USA) and the water vapor and CO₂ densities were measured by open-path
130 infrared gas analyzers (Li-7500, LiCor Inc., USA). Covariances were calculated every half-hour
131 after removing spikes and using Reynolds block averaging. We calculated fluxes of heat, water
132 and CO₂ using the covariances and applying a 2D coordinate rotation and accounting for density
133 effects. Net ecosystem exchange of CO₂ (NEE) was computed by adding the 30 minute change
134 in CO₂ storage term to the carbon dioxide flux. The storage term was estimated by using on the
135 change in concentration measured by the IRGA at the top of the towers. At the two taller
136 towers (MON1 and MON2) where profile measurements of CO₂ were available for part of the
137 records, this simple method of only using the change in IRGA concentration was shown to
138 produce negligible error (Scott et al., 2010; Scott et al., 2009).

1
2
3
4 139 The flux data were filtered for spikes, instrument malfunctions, and poor quality. Rejection
5
6
7 140 criteria used to screen data were: rain events, out-of-range signals, and spikes with the
8
9
10 141 standard deviation of [CO₂], [H₂O] and/or sonic temperature. The amount of missing 30-
11
12 142 minute NEE data for the entire period of data was 8.8%, 11.3%, 25.3%, and 37.4% at MON1,
13
14 143 MON2, MED1, and MED2, respectively, with more frequent gaps during periods of precipitation
15
16
17 144 and cold temperatures. Also, we applied published friction velocity (u^*) thresholds (0.15 m s^{-1} -
18
19
20 145 MON1 and MON2, 0.10 m s^{-1} - MED1, 0.20 m s^{-1} - MED2) to omit NEE fluxes when there was
21
22 146 not sufficient turbulence to make representative flux measurements (Malhi et al., 1998).
23
24
25 147 Applying the u^* threshold eliminated 7.0/21.8%, 13.4/43.2%, 3.4/20.2%, and 11.5/32.7%
26
27
28 148 (day/night) of the remaining NEE data at MON1, MON2, MED1, and MED2, respectively.
29
30
31 149 There are several techniques commonly used to gap-fill and partition EC-derived NEE. Each
32
33
34 150 technique introduces its own significant systematic error, yet despite this the overall temporal
35
36 151 patterns of the partitioned fluxes (gross ecosystem production, GEP, and ecosystem respiration,
37
38
39 152 R) and their magnitudes relative to each other remain robust regardless of technique (Lasslop
40
41 153 et al., 2010). Accordingly, we focus herein on these temporal patterns at each site and their
42
43
44 154 relative magnitudes between the sites rather than absolute magnitudes in our analysis below.
45
46
47 155 We partitioned NEE into R and GEP by first determining 30-minute R by fitting an exponential
48
49
50 156 function to air temperature and nighttime NEE data over a moving ~ 5 -day window (Reichstein
51
52 157 et al., 2005), where the window position and size were adjusted to ensure that data from pre-
53
54
55 158 rain (dry) periods were not grouped together with data following storms. This model was then
56
57
58 159 used to fill missing nighttime NEE data and model daytime respiration. Missing daytime values
59
60
61
62
63
64
65

1
2
3
4 160 of NEE were filled by fitting a 2nd order polynomial to the response of NEE to PAR for morning
5
6
7 161 and afternoon periods, separately, over a 5-day moving window. If the window contained less
8
9
10 162 than 60 values of NEE (roughly one half of the data potentially available in five days) the
11
12 163 window was incrementally increased one day at a time until this condition was met. Finally,
13
14 164 GEP was determined by $GEP = R - NEE$. We used the standard sign convention for NEE with
15
16
17 165 $NEE > 0$ indicating a net loss of CO₂ to the atmosphere (source) and $NEE < 0$ indicating CO₂
18
19
20 166 uptake by the ecosystem (sink). R and GEP are always positive. After computing daily sums of
21
22 167 these quantities there were cases where daily GEP was negative. This indicated an
23
24
25 168 underestimation of daily R so on these occasions GEP was zeroed with the magnitude of that
26
27
28 169 negative quantity added back into R. In the case of MED1 and MED2 where there is evidence of
29
30 170 CO₂ ventilation from rock and soil cavities (Rey et al., 2012; Sanchez-Cañete et al., 2011;
31
32
33 171 Serrano-Ortiz et al., 2009), this daily partitioning process captures the effects of this process on
34
35 172 the daily magnitude of R, but not its sub-daily temporal dynamics. However, it is because of this
36
37
38 173 process that we did not compare R between sites below. Linear regression was used to
39
40
41 174 determine the strength of the relationship between GEP and precipitation during spring (1-
42
43 175 January – 31-May) and summer (15-June – 31 October) at the monsoon sites, and 1-September
44
45
46 176 – 1-August at the Mediterranean sites. These periods were chosen based on overall patterns of
47
48 177 GEP shown at these sites (see next section). Specific pair-wise slope comparisons were made
49
50
51 178 using Tukey's Honestly Significant Difference (HSD) test, if F-test criteria testing for slope
52
53 179 differences described in Zar (Zar, 1974) were met. Standard errors to calculate HSD were made
54
55
56 180 using the pooled sum of squares, with HSD scores needing to exceed 5.35 to be significant at p
57
58
59 181 < 0.01.

1
2
3
4
5
6
7
8
9
10
11
12
13
14
15
16
17
18
19
20
21
22
23
24
25
26
27
28
29
30
31
32
33
34
35
36
37
38
39
40
41
42
43
44
45
46
47
48
49
50
51
52
53
54
55
56
57
58
59
60
61
62
63
64
65

182 As a measure of atmospheric evaporative demand, we computed the reference crop
183 evaporation rate, ET_o (Shuttleworth, 1993). Reference crop evaporation is an estimate of the
184 evaporation, which would occur from a short, well-watered grass with a fixed-height of 0.12 m,
185 an albedo of 0.23 and a surface resistance of 69 s m^{-1} .

186 As detailed site vegetation measurements to quantify phenological changes were not routinely
187 sampled at the sites, we used National Aeronautics and Space Administration's (NASA)
188 Moderate Resolution Imaging Spectroradiometer (MODIS) Enhanced Vegetation Index (EVI,
189 (Huete et al., 2002)), which was available as a composite 16-day, 250 m product (MOD13Q1;
190 ORNL DAAC, 2011) as a measure of vegetation greenness and phenological activity over the
191 course of this study at each site. EVI was averaged over the 9 pixels (a $0.75 \times 0.75 \text{ km}$ square)
192 around and centered on the tower.

193 Results

194 *Meteorological and phenological conditions*

195 The seasonal cycle of air temperature at all of these northern latitude sites was similar, but the
196 higher latitude/elevation MED2 was clearly cooler (Fig. 1). The rest of the sites were all cool in
197 winter, while the monsoon sites were considerably warmer in the summer, especially in May
198 and June prior to onset of the summer monsoon. The seasonality of precipitation was clearly
199 opposite with monsoon sites peaking in summer and Mediterranean sites in winter (Fig. 1).
200 Precipitation variability was high, and annual totals ranged between 230 – 404 mm at MON1,
201 162 -335 mm at MON2, 262 – 378 mm at MED1 and 182 – 1143 mm at MED2. MED2 was the
202 only site that had occasional periods of precipitation falling as snow in the winter months. But

1
2
3
4
5
6
7
8
9
10
11
12
13
14
15
16
17
18
19
20
21
22
23
24
25
26
27
28
29
30
31
32
33
34
35
36
37
38
39
40
41
42
43
44
45
46
47
48
49
50
51
52
53
54
55
56
57
58
59
60
61
62
63
64
65

203 these were storm specific, and the snow typically melted within a few days after the storm. The
204 monsoon sites had a higher atmospheric evaporative demand, as quantified by ET_0 (Fig. 1),
205 primarily due to higher solar radiation and vapor pressure deficit. The ratio P/ET_0 was always
206 less than unity at the monsoon sites indicating that these sites were always water-limited at the
207 monthly timescale, while $P/ET_0 > 1$ for the months of November through February at the
208 Mediterranean sites. Vegetation greenness, as quantified by EVI (Fig. 1), differed considerably
209 among the sites, especially at the Mediterranean ones. At MON1, EVI was higher than, but had
210 a very similar annual cycle to, MON2. At MED1, EVI increased monotonically over the fall
211 months, peaked in February/March, then decreased to minimum levels in the summer. At
212 MED2, EVI increased slightly in fall, bottomed out again from December through February,
213 ramped up to a peak EVI in May, and then declined to low values in August and September.

214 *NEE and GEP*

215 The seasonal patterns of NEE at the monsoon sites were very similar (Fig. 2) with little winter
216 activity, occasional springtime net uptake ($NEE < 0$), and inactive dry fore-summers. The periods
217 of spring net uptake at MON2 tended to begin and end earlier than at MON1, likely because the
218 mesquite trees at MON1 are less freeze tolerant and green-up later than perennial grasses. The
219 start of the monsoon around July result in periods of net efflux followed by peaks in uptake in
220 August and September that taper off in the drier and cooler fall months.

221 The patterns of NEE at the Mediterranean sites reveal short and highly variable periods of low
222 net uptake in winters and peak springtime uptake (Fig. 2). At MED1, periods of net uptake
223 began in mid-October and sometimes continued on through spring, a pattern which occurred

1
2
3
4
5
6
7
8
9
10
11
12
13
14
15
16
17
18
19
20
21
22
23
24
25
26
27
28
29
30
31
32
33
34
35
36
37
38
39
40
41
42
43
44
45
46
47
48
49
50
51
52
53
54
55
56
57
58
59
60
61
62
63
64
65

224 rarely at MED2. The spring net uptake peaks were larger and occurred later at the wetter and
225 colder MED2, where spring temperatures lagged behind MED1 by around two months. The dry
226 and hot summer months were characterized by net releases of CO₂.

227 Disaggregating NEE into its component fluxes, allows us to see the role that plants, as
228 quantified by GEP, contributed to the patterns of net CO₂ flux at these sites. At the monsoon
229 sites, there were both occasional spring and regular summer/fall growing seasons (Fig. 3), while
230 periods of net uptake (Fig. 2) were more limited and almost always lagged behind the onset of
231 significant vegetation growth (photosynthesis) especially in summer. At the Mediterranean
232 sites, photosynthesis usually began in fall and extended into spring or even early summer, but
233 GEP was lower and more discontinuous across the fall and winter at the higher and colder
234 MED2 site. In spring, the peak in mean GEP at MED1 was slightly broader and occurred earlier
235 than at MED2. These ensemble patterns of GEP were quite similar to the phenological patterns
236 (Fig. 1-EVI)

237 To demonstrate the role of water availability and temperature on vegetation growth and
238 carbon uptake at these sites, we selected two example years representing dry and wet
239 conditions from each site. Based on the patterns of flux activity shown at the sites (Fig. 2 and 3),
240 we display two calendar years for monsoon sites and two year length records beginning on the
241 1st of September for the Mediterranean sites. The latter is analogous to the concept of a
242 “hydrological year” commonly used in Mediterranean and snowmelt-dominated systems.

243 At the monsoon sites in 2006, there was a severe drought prior to the monsoon and an above-
244 average monsoon rain totals, and 2010 had above-average cool season rainfall and an average

1
2
3
4 245 monsoon (Fig. 4 and 5). In 2006, there was little GEP and NEE before monsoon onset.
5
6
7 246 Significant photosynthesis began about a week after the larger rains at the end of July. At the
8
9
10 247 monsoon onset, there was a large respiratory efflux ($NEE > 0$) and the period of net uptake did
11
12 248 not occur until after GEP was greater than ~ 2.5 (MON1) and $2.0 \text{ gC m}^{-2} \text{ d}^{-1}$ (MON2). Likewise, it
13
14
15 249 ended at a similar level of GEP, which peaked and declined shortly after the bulk of the
16
17 250 monsoon rainfall had ended. In 2010 there was a similar pattern of response during the
18
19
20 251 monsoon, but this El Niño year's wet cool season brought about sustained periods of
21
22 252 photosynthesis and net uptake in spring. The response of the vegetation in the spring was
23
24
25 253 different than in the monsoon as it lagged much farther behind the rainfall. Also, net uptake
26
27
28 254 did not lag far beyond the onset of photosynthesis to the same degree as it had in the monsoon
29
30 255 seasons. The spring onset of photosynthesis, defined $GEP > 0$ for five consecutive days, did not
31
32
33 256 begin until the temperature exceeded $7.0 \text{ }^\circ\text{C}$, quantified by the 10-day average daily
34
35 257 temperature prior to onset (T_{10}). Across all years, T_{10} averaged 12.2°C at MON1 and 7.3°C at
36
37
38 258 MON2 . While the seasonal patterns of GEP and NEE for these years at the monsoon sites were
39
40
41 259 broadly similar, NEE was usually higher at MON1, indicating less net CO_2 uptake overall (Scott et
42
43 260 al., 2009). Also, although there was considerably more cool-season precipitation at MON1 in
44
45
46 261 2010, the spring GEP and net uptake response were smaller.
47
48
49 262 At MED1, GEP responded immediately to the onset of fall rains, and the larger amount of early
50
51
52 263 rainfall in 2007-2008 gave rise to a longer and more vigorous winter of photosynthesis (Fig. 6).
53
54
55 264 While '08-'09 precipitation totals eventually caught up and then exceeded '07-'08 totals, this
56
57 265 was not until temperatures had declined. Photosynthesis continued to decline from December
58
59
60 266 2008 until February 2009 despite the additional water, and more substantial photosynthesis
61
62
63
64
65

1
2
3
4 267 occurred in the spring of 2009 only after average temperatures had warmed (mean $T_{10} = 10.6$
5
6
7 268 °C). With little precipitation in the spring of 2008, photosynthesis ceased in early April (Fig. 6).
8
9
10 269 However a large 40 mm pulse in May brought about significant vegetation growth for another
11
12 270 month. Periods of uptake were brief at this site and did not generally occur until GEP exceeded
13
14 271 $\sim 1.5 \text{ gC m}^{-2} \text{ d}^{-1}$.

16
17
18 272 At MED2, precipitation totals were low in 2004-2005 and very high in 2009-2010 (Fig. 7). In
19
20
21 273 autumn, photosynthesis began shortly after the arrival of rainfall in both years. Precipitation
22
23 274 was high enough in 2009 to generate a period of considerable GEP and net uptake, which were
24
25
26 275 quickly truncated by winter storms that brought large amounts of precipitation and cooler
27
28
29 276 temperatures near the end of December (Fig. 7). In the spring of both years, longer periods of
30
31 277 photosynthesis began in March –April, associated with an average $T_{10} = 5.6 \text{ °C}$. Here, periods of
32
33
34 278 significant uptake generally did not lag behind periods of vegetation growth and were
35
36 279 associated with a lower GEP threshold of $\sim 0.5 \text{ gC m}^{-2} \text{ d}^{-1}$.

37
38
39
40 280 *Precipitation and Photosynthesis*

41
42
43 281 Seasonal GEP was closely tied to precipitation at all sites (Fig. 8; all regressions significant at
44
45
46 282 $p < 0.05$), with significant GEP:P slope differences both within and between sites ($F_{5,25} = 26.5$;
47
48
49 283 $p < 0.05$). Pairwise Tukey's HSD testing shows this was due to MON1's springtime
50
51 284 photosynthetic sensitivity to precipitation being significantly lower than in summer at this site
52
53
54 285 and at MED1 (Fig. 8). The sensitivity for MON1-summer, MON2-both seasons, and MED1 did
55
56 286 not significantly differ, while it was lower than all others at MED2 (Fig. 8).

57
58
59
60 287 Discussion

1
2
3
4
5
6
7
8
9
10
11
12
13
14
15
16
17
18
19
20
21
22
23
24
25
26
27
28
29
30
31
32
33
34
35
36
37
38
39
40
41
42
43
44
45
46
47
48
49
50
51
52
53
54
55
56
57
58
59
60
61
62
63
64
65

288 We examined land-atmosphere carbon exchange from semiarid monsoon and Mediterranean
289 sites in order to examine how precipitation seasonality influences seasonal patterns of CO₂
290 fluxes. The variability of annual precipitation, especially relative to the mean, in dryland regions
291 is well known (Goodrich et al., 2008; Lázaro et al., 2001), and the importance of this variability
292 to ecosystem-level gas exchange is manifested because of prevailing water-limited status of
293 plants and microbes in these systems (Jenerette et al., 2011). While, as expected, the
294 variability in precipitation drove the large interannual variation in NEE and GEP at every site
295 (Fig. 1, 2, 3), there were commonalities in the flux responses across the dominant rainfall
296 regimes that depended on the precipitation seasonality.

297 We hypothesized that our monsoon sites would exhibit a characteristic Mediterranean
298 response given sufficient cool-season precipitation. This was supported by the presence of
299 significant GEP and net CO₂ uptake in the spring (Fig. 2 and 3) that was not an immediate
300 response to recent precipitation and rather a response to warming temperatures (and/or light)
301 and precipitation that had accumulated in the soil much earlier (Fig. 4 and 5). Previous studies
302 have analyzed seasonal and annual variability of CO₂ fluxes at the individual semiarid monsoon
303 sites used in this study (Scott et al., 2010; Scott et al., 2009) and elsewhere (Eamus et al., 2001;
304 Hastings et al., 2005; Kurc and Small, 2007; Leuning et al., 2005; Perez-Ruiz et al., 2010). In
305 concurrence with smaller datasets (Scott et al., 2010; Scott et al., 2009), the annual cycles of
306 GEP and NEE at MON1 and MON2 indicate a dominant annual growing season and period of net
307 uptake governed by the timing and the strength of the North American Monsoon and a
308 separate, but occasional, growing season in spring given sufficient cool-season rainfall (Fig. 2
309 and 3). This mix of slow and delayed versus fast and immediate responses support Reynolds et

1
2
3
4
5
6
7
8
9
10
11
12
13
14
15
16
17
18
19
20
21
22
23
24
25
26
27
28
29
30
31
32
33
34
35
36
37
38
39
40
41
42
43
44
45
46
47
48
49
50
51
52
53
54
55
56
57
58
59
60
61
62
63
64
65

310 al. (2004), who suggested that the simple rainfall-pulse-then-biological-pulse-response is too
311 limited and should be modified to include the concept of pulses of soil moisture recharge which
312 are differentially utilized depending on plant functional types and site conditions (soil type,
313 meteorology). Also similar to the Mediterranean responses, the decrease in temperatures
314 and/or light in winter led to suppressed fluxes despite the occurrence of precipitation. This
315 behavior has been observed at other mid-latitude monsoon sites (Anderson-Teixeira et al.,
316 2011; Kurc and Small, 2007), but not at warmer, low latitude locations with higher winter
317 temperatures (Hastings et al., 2005).

318 While the general patterns of fluxes at the monsoon sites were quite similar, there were some
319 important differences. Springtime GEP was higher and NEE was lower in 2010 at MON2 even
320 with less antecedent P (Fig. 4 and 5), and this spring photosynthetic response at MON1 was
321 weaker throughout all the years of this study (Fig. 8). We speculate that this was due to the
322 denser herbaceous vegetation and higher water holding capacity of the clay-rich soils at MON2.
323 Also while during the main monsoon growing season GEP at MON1 is usually greater and more
324 sensitive to precipitation relative to MON2 (Fig. 3, 8), there tends to be less net CO₂ uptake (Fig.
325 2) that may be due to greater standing biomass stemming from differences in vegetation
326 composition (woody vs. herbaceous) that lead to higher respiration costs at MON1 (Scott et al.,
327 2010; Scott et al., 2009).

328 We also hypothesized that the Mediterranean sites would exhibit a characteristic monsoon
329 response, with immediate pulses of carbon flux activity (Huxman et al., 2004), when significant
330 precipitation falls in the non-winter season. This was supported by the rapid onset of fluxes

1
2
3
4 331 responding to the return of rainfall in autumn (Fig. 6 and 7) or even late spring rain events
5
6
7 332 (May, 2008, Fig. 6). Similarly, the large variability and seasonal timing in NEE shown at MED1
8
9
10 333 and MED2 in this study (Fig.2) are supported by previous studies (Rey et al., 2012; Serrano-Ortiz
11
12 334 et al., 2009). The length of the growing season is dominated by the amount and timing of
13
14 335 precipitation (Aires et al., 2008; Rey et al., 2012; Serrano-Ortiz et al., 2009; Xu and Baldocchi,
15
16
17 336 2004) and governs the interannual NEE variability (Ma et al., 2007). However, due to
18
19
20 337 differences in altitude and thus, differences in temperature, plant growth at the lower elevation
21
22 338 MED1 is more vigorous (Fig. 1-EVI and 3) during the fall and winter and can act as a carbon sink
23
24
25 339 during this period (Fig. 3), while growth was more limited in fall and especially winter at MED2,
26
27
28 340 where there was a distinct cessation of photosynthesis likely due to the colder temperatures
29
30 341 and occasional snowfall (Serrano-Ortiz et al., 2007). Thus, carbon accumulated ($NEE < 0$) more
31
32
33 342 often at the end of spring and continued till late summer at MED2 (Fig. 2). Seasonal
34
35 343 precipitation amounts also control the length of the dry period in summer. During the dry
36
37
38 344 period, the ecosystems acted as net sources, emitting the CO_2 probably due to a combination of
39
40
41 345 processes (respiration, photo-degradation, and ventilation from rock and soil cavities).
42
43
44 346 For these water-limited ecosystems, photosynthesis was strongly coupled to precipitation (Fig.
45
46
47 347 8). We hypothesized that the monsoon sites would be more responsive given the higher typical
48
49 348 growing season temperatures. This was partially supported in that response of GEP to
50
51
52 349 precipitation was significantly lower than the rest of the sites at MED2, but the sensitivity at
53
54 350 MED1 was not distinct from both MON1 (summer only) and MON2 (both seasons), suggesting a
55
56
57 351 similar ecosystem rain use efficiency (GEP/P). This is quite surprising given the differences in
58
59
60 352 the plant composition, structure, and soils between the sites (Table 1). However, it was also

1
2
3
4
5
6
7
8
9
10
11
12
13
14
15
16
17
18
19
20
21
22
23
24
25
26
27
28
29
30
31
32
33
34
35
36
37
38
39
40
41
42
43
44
45
46
47
48
49
50
51
52
53
54
55
56
57
58
59
60
61
62
63
64
65

353 clear that, even at one site (MON1, Fig. 8), rain use efficiency can clearly vary between the
354 spring and summer periods. While more investigation is needed, we suggest that the
355 diminished sensitivity at MON1 (spring) and MED2 may be due to similar reasons concerning
356 how cool-season precipitation is translated into springtime plant available soil moisture via site-
357 specific soil properties. Temperatures and/or light appear to limit plant activity during winter
358 at MON1 and MED2 (Fig. 3, 4, 7), precipitation that falls during this time may quickly infiltrate
359 past the root zone in the very sandy soils (MON1) or drained (groundwater recharge) by the
360 karst terrain (MED2) before the plants can utilize this water in the subsequent growing season
361 (Cantón et al., 2010).

362 Finally, while precipitation was the dominant control, the depression in energy input in the
363 winter at these mid-latitude sites also played a governing seasonal role (Fig. 4-7). Starting
364 dates of springtime photosynthesis had antecedent temperatures (T_{10}) that declined from
365 $\sim 12^{\circ}\text{C}$ at the warmest MON1 site to the $\sim 6^{\circ}\text{C}$ at coolest MED2 site, suggesting some thermal
366 adaptation of ecosystem photosynthesis (Baldocchi et al., 2001; Yuan et al., 2011).

367 Temperature also likely played an important role in determining when periods of
368 photosynthesis transitioned into periods of net uptake. At the monsoon sites, this transition
369 was reached when GEP increased above $\sim 1 \text{ gC m}^{-2} \text{ d}^{-1}$ in the spring and $\sim 2 - 2.5 \text{ gC m}^{-2} \text{ d}^{-1}$ in the
370 summer (Fig. 4 and 5). Periods of net uptake occurred when GEP was above $\sim 0.5 \text{ gC m}^{-2} \text{ d}^{-1}$ in
371 the spring at MED2 and $\sim 1 - 1.5 \text{ gC m}^{-2} \text{ d}^{-1}$ in the fall at MED1 (Fig. 6 and 7). The magnitude of
372 these GEP thresholds increase with temperature at the sites probably due to the strong positive
373 relationship between temperature and respiration, which must be exceeded by GEP to have net
374 uptake.

1
2
3
4 375 Conclusions
5
6
7

8 376 In this comparison of semiarid sites dominated by differences in winter and summer
9
10 377 precipitation, many commonalities in the response of CO₂ fluxes to atmospheric forcing were
11
12
13 378 observed. Precipitation magnitude and timing were the dominant drivers of carbon exchange,
14
15 379 but temperature also played an important role in regulating gross and net ecosystem carbon
16
17
18 380 uptake at all sites. Also, the fluxes rapidly responded to precipitation events in a pulsed manner
19
20
21 381 (even at the Mediterranean sites) but mainly in the warm season when temperatures were not
22
23 382 limiting. In the coolest parts of the winter season, photosynthesis and uptake were not
24
25
26 383 responsive to precipitation. Rather, precipitation accumulated in the soil and fueled springtime
27
28
29 384 growth after it had warmed. Cumulative photosynthesis was strongly related to precipitation
30
31 385 within and across sites. The site-specific differences like the magnitude and timing of the
32
33
34 386 periods of photosynthesis and net CO₂ uptake are likely related to the differences in site
35
36 387 composition (e.g., MON2 - grass and MON1 - mixed grass and tree), soils (e.g., low versus high
37
38
39 388 soil water holding capacity) and atmospheric forcing (e.g., temperature differences between
40
41 389 MED2 and the other sites). Together, these results support a more unified conceptual model of
42
43
44 390 carbon cycling in semiarid ecosystems, such that the description of the ecosystem processes
45
46
47 391 that contribute to carbon exchanges need not differ between warm-season and cool-season
48
49 392 rainfall regimes. Using the modified Pulse Paradigm of Reynolds et al. (2004), pulses of soil
50
51
52 393 moisture recharge are acted upon by biology (plants and microbes) to generate pulses on
53
54 394 carbon flux responses, whose timing and magnitude depends on environmental triggers like
55
56
57 395 temperature and light.
58
59
60
61
62
63
64
65

1
2
3
4
5
6
7
8
9
10
11
12
13
14
15
16
17
18
19
20
21
22
23
24
25
26
27
28
29
30
31
32
33
34
35
36
37
38
39
40
41
42
43
44
45
46
47
48
49
50
51
52
53
54
55
56
57
58
59
60
61
62
63
64
65

396 Acknowledgements

397 This paper is the result of a fellowship funded by the OECD Co-operative Research Programme:
398 Biological Resource Management for Sustainable Agricultural Systems to R.L. Scott. This paper
399 has been supported in part by the Andalusian regional government project GEOCARBO and
400 GLOCHARID (P08-RNM-3721), European Union Funds (ERDF and ESF), the Spanish flux-tower
401 network CARBORED-ES (Science Ministry project CGL2010-22193-C04-02), and the European
402 Commission collaborative project GHG Europe (FP7/2007-2013; grant agreement 244122).
403 USDA is an equal opportunity employer.

1
2
3
4
5
6
7
8
9
10
11
12
13
14
15
16
17
18
19
20
21
22
23
24
25
26
27
28
29
30
31
32
33
34
35
36
37
38
39
40
41
42
43
44
45
46
47
48
49
50
51
52
53
54
55
56
57
58
59
60
61
62
63
64
65

404 References

405 Aires, L.M.I., Pio, C.A., Pereira, J.S., 2008. Carbon dioxide exchange above a Mediterranean C3/C4
406 grassland during two climatologically contrasting years. *Global Change Biol.* 14, 539-555,
407 doi:10.1111/j.1365-2486.2007.01507.x.

408 Anderson-Teixeira, K.J., Delong, J.P., Fox, A.M., Brese, D.A., Litvak, M.E., 2011. Differential responses of
409 production and respiration to temperature and moisture drive the carbon balance across a
410 climatic gradient in New Mexico. *Global Change Biol.* 17, 410-424, doi:10.1111/j.1365-
411 2486.2010.02269.x.

412 Baldocchi, D., Falge, E., Gu, L., Olson, R., Hollinger, D., Running, S., Anthoni, P., Bernhofer, C., Davis, K.,
413 Evans, R., Fuentes, J., Goldstein, A., Katul, G., Law, B., Lee, X., Malhi, Y., Meyers, T., Munger, W.,
414 Oechel, W., Paw, U.K.T., Pilegaard, K., Schmid, H.P., Valentini, R., Verma, S., Vesala, T., Wilson,
415 K., Wofsy, S., 2001. FLUXNET: A New Tool to Study the Temporal and Spatial Variability of
416 Ecosystem-Scale Carbon Dioxide, Water Vapor, and Energy Flux Densities. *Bull. Am. Meteorol.*
417 *Soc.* 82, 2415-2434.

418 Cantón, Y., Villagarcía, L., Moro, M.J., Serrano-Ortíz, P., Were, A., Alcalá, F.J., Kowalski, A.S., Solé-Benet,
419 A., Lázaro, R., Domingo, F., 2010. Temporal dynamics of soil water balance components in a
420 karst range in southeastern Spain: estimation of potential recharge. *Hydrological Sciences*
421 *Journal* 55, 737-753.

422 Eamus, D., Hutley, L.B., O'Grady, A.P., 2001. Daily and seasonal patterns of carbon and water fluxes
423 above a north Australian savanna. *Tree Physiol.* 21, 977-988.

424 Emmerich, W.E., 2003. Carbon dioxide fluxes in a semiarid environment with high carbonate soils. *Agric.*
425 *For. Meteorol.* 116, 91-102.

426 Emmerich, W.E., 2007. Ecosystem water use efficiency in a semiarid shrubland and grassland
427 community. *Rangeland Ecology and Management* 60, 464-470.

428 Eswaran, H., Reich, P.F., Kimble, J.M., Beinroth, F.H., Padmanabham, E., Moncharoen, P., 2000. Global
429 carbon stocks. In: R. Lal, J.M. Kimble, H. Eswaran and B.A. Stewart (Editors), *Global climate*
430 *change and pedogenic carbonates*. Lewis Publishers, Boca Raton, FL.

431 Goodrich, D.C., Unkrich, C.L., Keefer, T.O., Nichols, M.H., Stone, J.J., Levick, L.R., Scott, R.L., 2008. Event
432 to multidecadal persistence in rainfall and runoff in southeast Arizona. *Water Resour. Res.* 44,
433 W05S14.

1
2
3
4 434 Hastings, S.J., Oechel, W.C., Muhlia-Melo, A., 2005. Diurnal, seasonal and annual variation in the net
5 435 ecosystem CO₂ exchange of a desert shrub community (*Sarcocaulis*) in Baja California,
6 436 Mexico. *Global Change Biol.* 11, 927-939, doi:10.1111/j.1365-2486.2005.00951.x.
7
8
9
10 437 Huete, A., Didan, K., Miura, T., Rodriguez, E.P., Gao, X., Ferreira, L.G., 2002. Overview of the radiometric
11 438 and biophysical performance of the MODIS vegetation indices. *Remote Sens. Environ.* 83, 195-
12 439 213, doi:10.1016/S0034-4257(02)00096-2.
13
14
15 440 Huxman, T.E., Snyder, K.A., Tissue, D., Leffler, A.J., Ogle, K., Pockman, W.T., Sandquist, D.R., Potts, D.L.,
16 441 Schwinning, S., 2004. Precipitation pulses and carbon fluxes in semiarid and arid ecosystems.
17 442 *Oecologia* 141, 254-268, doi:10.1007/s00442-004-1682-4.
18
19
20
21 443 Jenerette, G.D., Barron-Gafford, G.A., Guswa, A.J., McDonnell, J.J., Villegas, J.C., 2011. Organization of
22 444 complexity in water limited ecohydrology. *Ecohydrology* in press, doi:10.1002/eco.217.
23
24
25
26 445 Kurc, S.A., Small, E.E., 2007. Soil moisture variations and ecosystem-scale fluxes of water and carbon in
27 446 semiarid grassland and shrubland. *Water Resour. Res.* 43, W06416,
28 447 doi:10.1029/2006WR005011.
29
30
31 448 Lal, R., 2004. Carbon sequestration in dryland ecosystems. *Environ. Manag.* 33, 528-544.
32
33
34
35 449 Lasslop, G., Reichstein, M., Papale, D., Richardson, A., Arneeth, A., Barr, A., Stoy, P., Wohlfahrt, G., 2010.
36 450 Separation of net ecosystem exchange into assimilation and respiration using a light response
37 451 curve approach: Critical issues and global evaluation. *Global Change Biol.* 16, 187-208,
38 452 doi:10.1111/j.1365-2486.2009.02041.x.
39
40
41 453 Lázaro, R., Rodrigo, F.S., Gutiérrez, L., Domingo, F., Puigdefábregas, J., 2001. Analysis of a 30-year rainfall
42 454 record (1967-1997) in semi-arid SE Spain for implications on vegetation. *J. Arid Environ.* 48, 373-
43 455 395.
44
45
46
47 456 Leuning, R., Cleugh, H.A., Zegelin, S.J., Hughes, D., 2005. Carbon and water fluxes over a temperate
48 457 Eucalyptus forest and a tropical wet/dry savanna in Australia: Measurements and comparison
49 458 with MODIS remote sensing estimates. *Agric. For. Meteorol.* 129, 151-173,
50 459 doi:10.1016/j.agrformet.2004.12.004.
51
52
53
54 460 Luo, H., Oechel, W.C., Hastings, S.J., Zulueta, R., Qian, Y., Kwon, H., 2007. Mature semiarid chaparral
55 461 ecosystems can be a significant sink for atmospheric carbon dioxide. *Global Change Biol.* 13,
56 462 386-396, doi:10.1111/j.1365-2486.2006.01299.x.
57
58
59
60
61
62
63
64
65

1
2
3
4 463 Ma, S., Baldocchi, D.D., Xu, L., Hehn, T., 2007. Inter-annual variability in carbon dioxide exchange of an
5 464 oak/grass savanna and open grassland in California. *Agric. For. Meteorol.* 147, 157-171.
6
7
8
9 465 Malhi, Y., Nobre, A.D., Grace, J., Kruijt, B., Pereira, M.G.P., Culf, A., Scott, S., 1998. Carbon dioxide
10 466 transfer over a Central Amazonian rain forest. *J. Geophys. Res. [Atmos.]* 103, 31593-31612.
11
12
13 467 Mielnick, P., Dugas, W.A., Mitchell, K., Havstad, K., 2005. Long-term measurements of CO₂ flux and
14 468 evapotranspiration in a Chihuahuan desert grassland. *J. Arid Environ.* 60, 423-436,
15 469 doi:10.1016/j.jaridenv.2004.06.001.
16
17
18
19 470 Noy-Meir, I., 1973. Desert ecosystems: Environment and producers. *Annu. Rev. Ecol. Syst.* 4, 25-51,
20 471 doi:doi:10.1146/annurev.es.04.110173.000325.
21
22
23 472 Oak Ridge National Laboratory Distributed Active Archive Center (ORNL DAAC). 2011. MODIS
24 473 subsetted land products, Collection 5. Available on-line
25 474 [<http://daac.ornl.gov/MODIS/modis.html>] from ORNL DAAC, Oak Ridge, Tennessee,
26 475 U.S.A. Accessed January 20, 2011.
27
28
29 476 Perez-Ruiz, E.R., Garatuza-Payan, J., Watts, C.J., Rodriguez, J.C., Yezpez, E.A., Scott, R.L., 2010. Carbon
30 477 dioxide and water vapour exchange in a tropical dry forest as influenced by the North American
31 478 Monsoon System (NAMS). *J. Arid Environ.* 74, 556-563, doi:10.1016/j.jaridenv.2009.09.029.
32
33
34
35 479 Rasmussen, C., 2006. Distribution of soil organic and inorganic carbon pools by biome and soil taxa in
36 480 Arizona. *Soil Sci. Soc. Am. J.* 70, 256-265.
37
38
39 481 Rey, A., Belelli-Marchesini, L., Were, A., Serrano-Ortiz, P., Etiope, G., Papale, D., Domingo, F., Pegoraro,
40 482 E., 2012. Wind as a main driver of the net ecosystem carbon balance of a semiarid
41 483 Mediterranean steppe in the South East of Spain. *Global Change Biol.* 18, 539-554,
42 484 doi:10.1111/j.1365-2486.2011.02534.x.
43
44
45
46 485 Reynolds, J.F., Kemp, P.R., Ogle, K., Fernandez, R.J., 2004. Modifying the 'pulse-reserve' paradigm for
47 486 deserts of North America: Precipitation pulses, soil water, and plant responses. *Oecologia* 141,
48 487 194-210.
49
50
51
52 488 Sanchez-Canete, E.P., Serrano-Ortiz, P., Kowalski, A.S., Oyonarte, C., Domingo, F., 2011. Subterranean
53 489 CO₂ ventilation and its role in the net ecosystem carbon balance of a karstic shrubland.
54 490 *Geophysical Research Letters* 38, L09802, doi:10.1029/2011GL047077
55
56
57
58 491 Schlesinger, W.H., Reynolds, J.F., Cunningham, G.L., Huenneke, L.F., Jarrell, W.M., Virginia, R.A.,
59 492 Whitford, W.G., 1990. Biological Feedbacks in Global Desertification. *Science* 247, 1043-1048,
60 493 doi:10.1126/science.247.4946.1043.
61
62
63
64
65

1
2
3
4 494 Scott, R.L., Hamerlynck, E.P., Jenerette, G.D., Moran, M.S., Barron-Gafford, G.A., 2010. Carbon dioxide
5 495 exchange in a semidesert grassland through drought-induced vegetation change. *J. Geophys.*
6 496 *Res.* 115, G03026, doi:10.1029/2010JG001348
7
8
9
10 497 Scott, R.L., Jenerette, G.D., Potts, D.L., Huxman, T.E., 2009. Effects of seasonal drought on net carbon
11 498 dioxide exchange from a woody-plant-encroached semiarid grassland. *J. Geophys. Res. [Biogeo.]*
12 499 114, G04004, doi:10.1029/2008JG000900.
13
14
15 500 Serrano-Ortiz, P., Domingo, F., Cazorla, A., Were, A., Cuezva, S., Villagarcia, L., Alados-Arboledas, L.,
16 501 Kowalski, A.S., 2009. Interannual CO₂ exchange of a sparse Mediterranean shrubland on a
17 502 carbonaceous substrate. *J. Geophys. Res. [Biogeo.]* 114, G04015, doi:10.1029/2009JG000983.
18
19
20
21 503 Serrano-Ortiz, P., Kowalski, A.S., Domingo, F., Rey, A., Pegoraro, E., Villagarcia, L., Alados-Arboledas, L.,
22 504 2007. Variations in daytime net carbon and water exchange in a montane shrubland ecosystem
23 505 in southeast Spain. *Photosynthetica* 45, 30-35, doi:10.1007/s11099-007-0005-5.
24
25
26
27 506 Serrano-Ortiz, P., Roland, M., Sanchez-Moral, S., Janssens, I.A., Domingo, F., Godderis, Y., Kowalski, A.S.,
28 507 2010. Hidden, abiotic CO₂ flows and gaseous reservoirs in the terrestrial carbon cycle: Review
29 508 and perspectives. *Agric. For. Meteorol.* 150, 321-329, doi:10.1016/j.agrformet.2010.01.002.
30
31
32
33 509 Shuttleworth, W.J., 1993. Evaporation. In: D.R. Maidment (Editor), *Handbook of Hydrology*. McGraw-Hill,
34 510 Inc., New York, pp. 4.1-4.53.
35
36
37 511 Small, E.E., Kurc, S.A., 2003. Tight coupling between soil moisture and the surface radiation budget in
38 512 semiarid environments: Implications for land-atmosphere interactions. *Water Resour. Res.* 39,
39 513 1278, doi:10.1029/2002WR001297.
40
41
42
43 514 Xu, L., Baldocchi, D.D., 2004. Seasonal variation in carbon dioxide exchange over a Mediterranean
44 515 annual grassland in California. *Agric. For. Meteorol.* 123, 79-96,
45 516 doi:10.1016/j.agrformet.2003.10.004.
46
47
48 517 Yuan, W., Luo, Y., Liang, S., Yu, G., Niu, S., Stoy, P., Chen, J., Desai, A.R., Lindroth, A., Gough, C.M.,
49 518 Ceulemans, R., Arain, A., Bernhofer, C., Cook, B., Cook, D.R., Dragoni, D., Gielen, B., Janssens,
50 519 I.A., Longdoz, B., Liu, H., Lund, M., Matteucci, G., Moors, E., Scott, R.L., Seufert, G., Varner, R.,
51 520 2011. Thermal adaptation of net ecosystem exchange. *Biogeosciences* 8, 1453-1463,
52 521 doi:10.5194/bg-8-1453-2011.
53
54
55
56 522 Zar, J.H., 1974. *Biostatistical Analysis*. Prentice-Hall, Englewood Cliffs, N.J., 215 pp.
57 523
58 524
59
60
61
62
63
64
65

525 Table 1. Physical description of the study sites.

Site Abbreviations and Names	MON1 Santa Rita Mesquite Savanna	MON2 Kendall Grassland	MED1 Balsablanca	MED2 El Llano de los Juanes
Location	Santa Rita Exp. Range Arizona, USA	Walnut Gulch Exp. Watershed Arizona, USA	Cabo de Gata Almería, Spain	Sierra de Gádor Almería, Spain
Data Period	Jan,2004 – Dec,2010	May,2004 – Dec,2010	Jun,2006 – Dec,2010	May,2004 – Dec,2010
Elevation (m)	1120	1530	195	1600
Mean Air Temperature (period of study, °C)	19.2	17.5	17.3	11.9
Annual precipitation (period of study, mm)	324	262	319	632
Ecosystem description and dominant species	Sonoran Desert upland, dry savanna with deciduous C ₃ mesquite trees (<i>Prosopis velutina</i>) and an understory of various perennial C ₄ bunchgrasses (<i>Eragrostis lehmanniana</i>), annual C ₄ grasses (<i>Bouteloua aristidoides</i>), and interspersed	Chihuahuan Desert upland, semidesert perennial C ₄ grassland (<i>Bouteloua spp.</i> until 2006 and <i>Eragrostis lehmanniana</i> after) interspersed with small shrubs and herbaceous annuals	Mediterranean steppe, 7 km from the coast, perennial C ₃ tussock grass (<i>Stipa tenacissima</i>) interspersed with other perennial species	Mediterranean shrubland plateau, 25 km from the coast, perennial C ₃ grasses (<i>Festuca scariosa</i>) and shrubs (<i>Genista pumila</i> , <i>Hormathophilla spinosa</i>)

1
2
3
4
5
6
7
8
9
10
11
12
13
14
15
16
17
18
19
20
21
22
23
24
25
26
27
28
29
30
31
32
33
34
35
36
37
38
39
40
41
42
43
44
45
46
47
48
49
50
51
52
53
54
55
56
57
58
59
60
61
62
63
64
65

	with various subshrubs and succulents			
Average canopy height (m)	2.5 (trees), 0.5 (grasses)	0.5	0.75	0.5
Peak Leaf Area Index and peak month	~1 (August)	~1 (August)	~1 (January)	~1 (May)
Vegetation coverage (%)	50 (total) with 35% tree cover	40	60	50
Soil depth and type	1-2 m, deep, loamy sands	1 – 2 m, deep, very gravelly, sandy to fine loams	0 – 0.3 m, thin sandy loams underlain by marine carbonate sediments	0-1.5 m, silt loams underlain by limestone bedrock

526
527

1
2
3
4
5
6
7
8
9
10
11
12
13
14
15
16
17
18
19
20
21
22
23
24
25
26
27
28
29
30
31
32
33
34
35
36
37
38
39
40
41
42
43
44
45
46
47
48
49
50
51
52
53
54
55
56
57
58
59
60
61
62
63
64
65

528 Figure Captions

529 Figure 1. Mean monthly air temperature, precipitation, reference crop evaporation (ET_o), and
530 MODIS Enhanced Vegetation Index (EVI) during the period of study. Error bars represent +/- 1
531 standard deviation from the mean, which are not shown for precipitation as they dwarf the
532 magnitude of the means.

533
534 Figure 2. Daily net ecosystem exchange of CO_2 (NEE) for all sites. Individual years are shown
535 along with the ensemble daily mean (thick solid line).

536 Figure 3. Daily gross ecosystem production (GEP) for all sites. Individual years are shown along
537 with the ensemble daily mean (thick solid line).

538 Figure 4. Two example calendar years of cumulative precipitation (P), daily average air
539 temperature (T_a), gross ecosystem production (GEP) and net ecosystem exchange (NEE) at
540 MON1.

541 Figure 5. Two example calendar years of cumulative precipitation (P), daily average air
542 temperature (T_a), gross ecosystem production (GEP) and net ecosystem exchange (NEE) at
543 MON2.

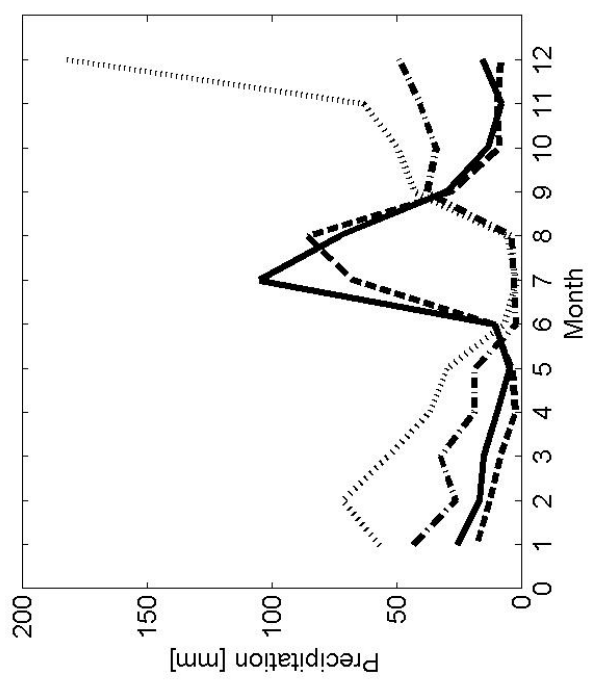
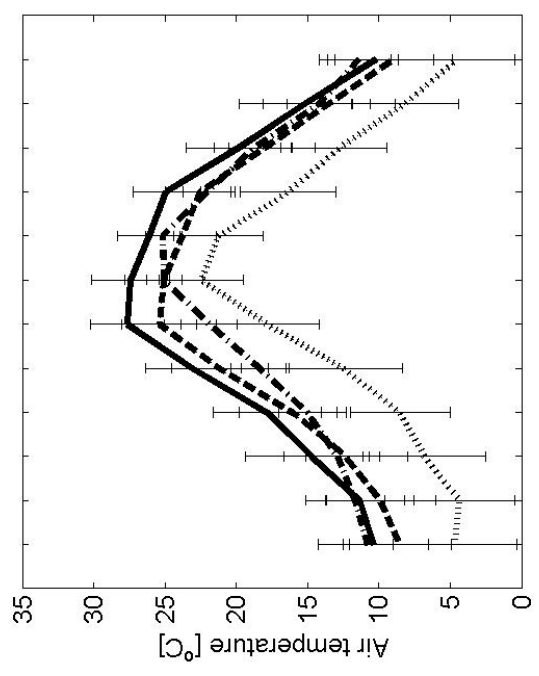
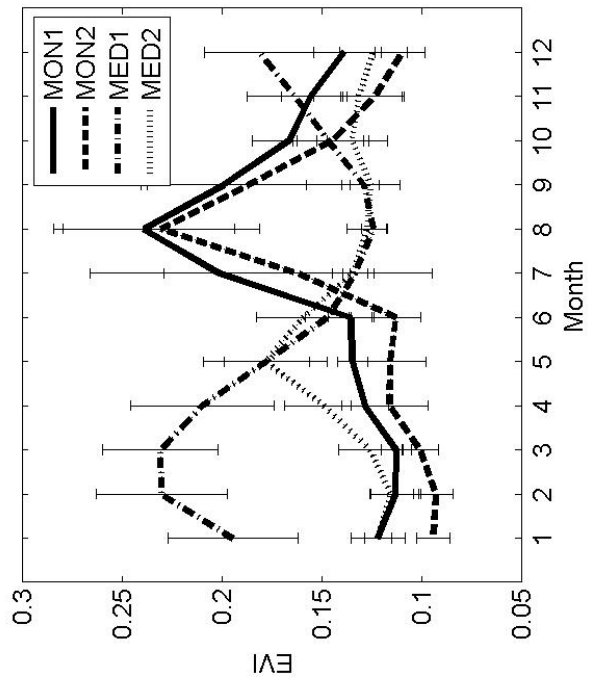
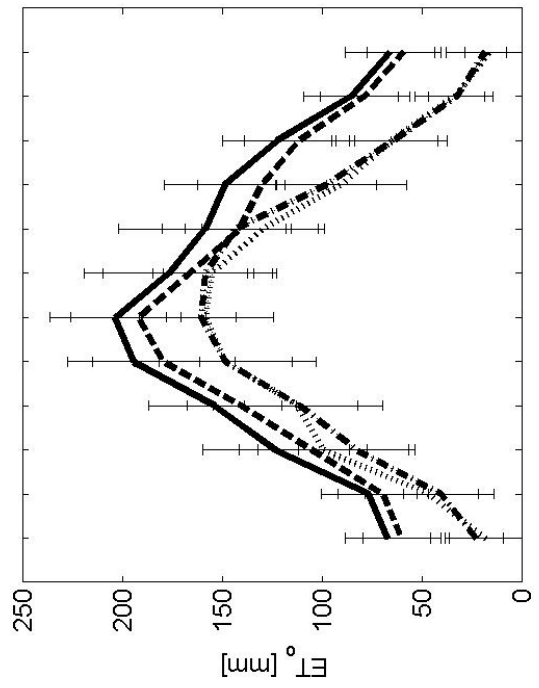
544 Figure 6. Two example hydrological years (September – August) of cumulative precipitation (P),
545 daily average air temperature (T_a), gross ecosystem production (GEP) and net ecosystem
546 exchange (NEE) at MED1.

1
2
3
4
5
6
7
8
9
10
11
12
13
14
15
16
17
18
19
20
21
22
23
24
25
26
27
28
29
30
31
32
33
34
35
36
37
38
39
40
41
42
43
44
45
46
47
48
49
50
51
52
53
54
55
56
57
58
59
60
61
62
63
64
65

547 Figure 7. Two example hydrological years (September – August) of cumulative precipitation (P),
548 daily average air temperature (T_a), gross ecosystem production (GEP) and net ecosystem
549 exchange (NEE) at MED2.

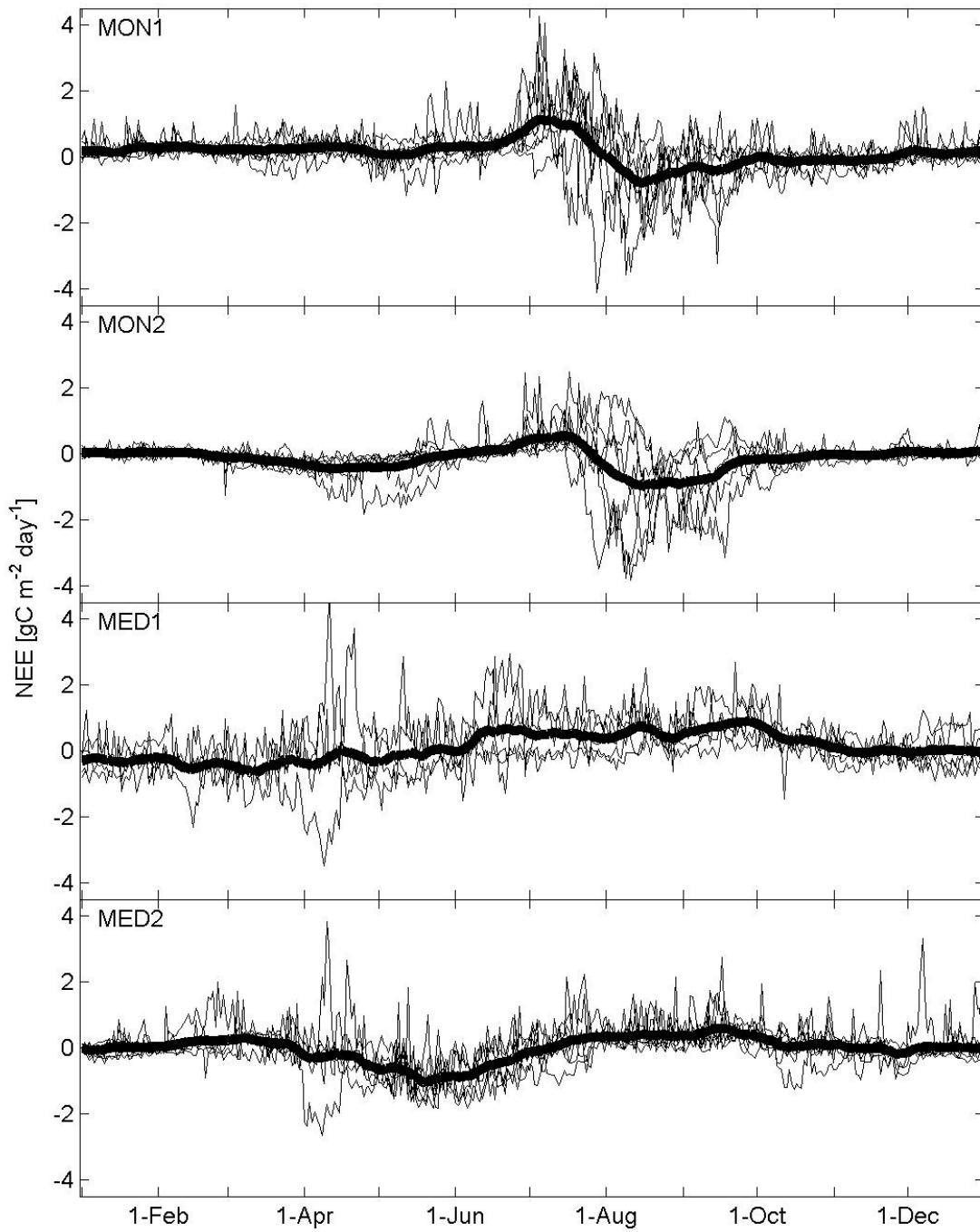
550 Figure 8. Total precipitation (P) and photosynthesis (GEP). For the monsoon sites, spring (1-
551 January – 31-May) and summer (15-June – 31 October) totals are separated due to the
552 seasonally distinct growing seasons. For the Mediterranean sites, only 1-September – 1-August
553 totals are shown. All least squares regressions are significant at $\alpha = 0.05$; regressions lacking a
554 common superscript letter have slopes differing significantly at $p < 0.05$ (Tukey HSD).

1
2
3
4
5
6
7
8
9
10
11
12
13
14
15
16
17
18
19
20
21
22
23
24
25
26
27
28
29
30
31
32
33
34
35
36
37
38
39
40
41
42
43
44
45
46
47
48
49
50
51
52
53
54
55
56
57
58
59
60
61
62
63
64
65



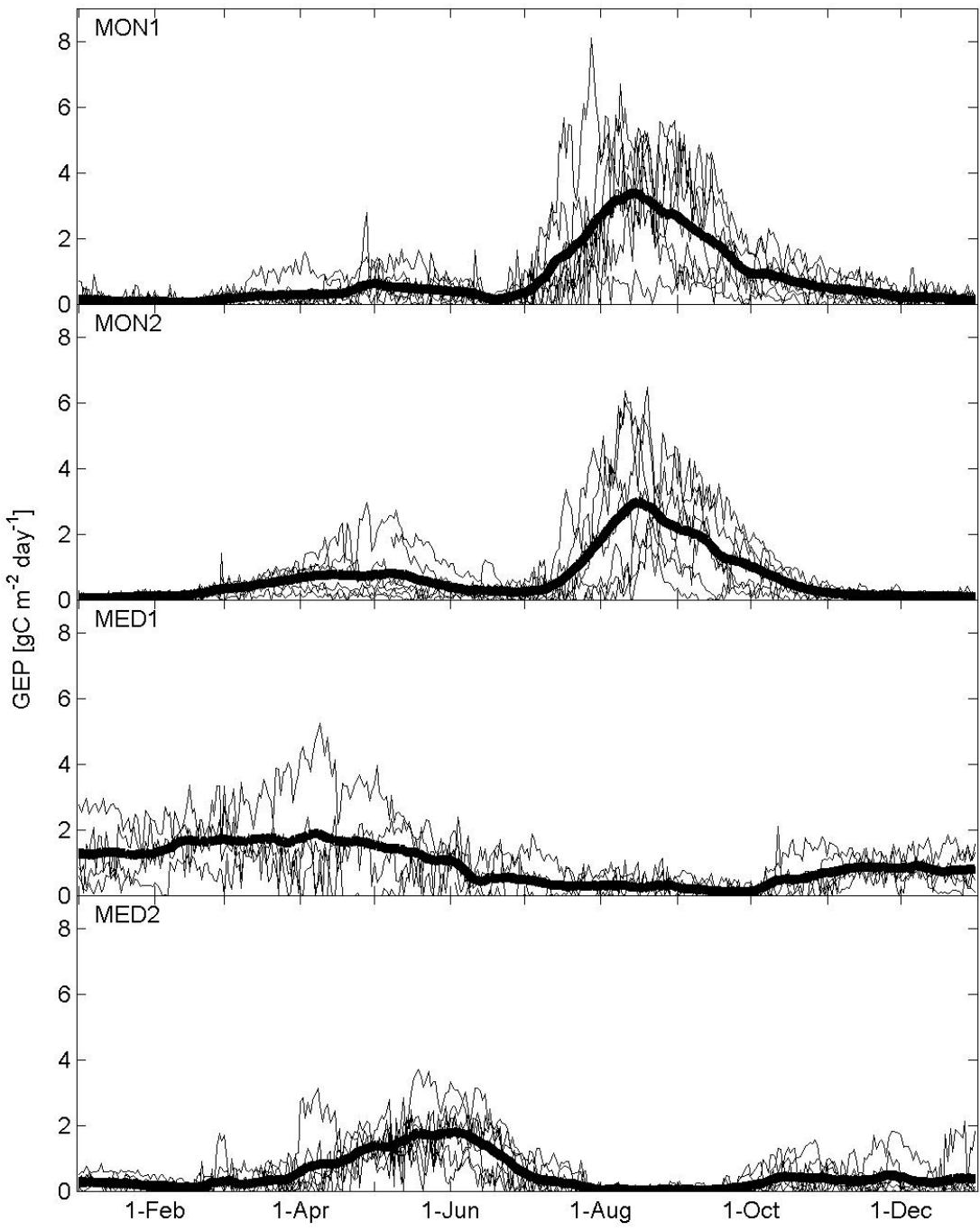
555

1
2
3
4
5
6
7
8
9
10
11
12
13
14
15
16
17
18
19
20
21
22
23
24
25
26
27
28
29
30
31
32
33
34
35
36
37
38
39
40
41
42
43
44
45
46
47
48
49
50
51
52
53
54
55
56
57
58
59
60
61
62
63
64
65



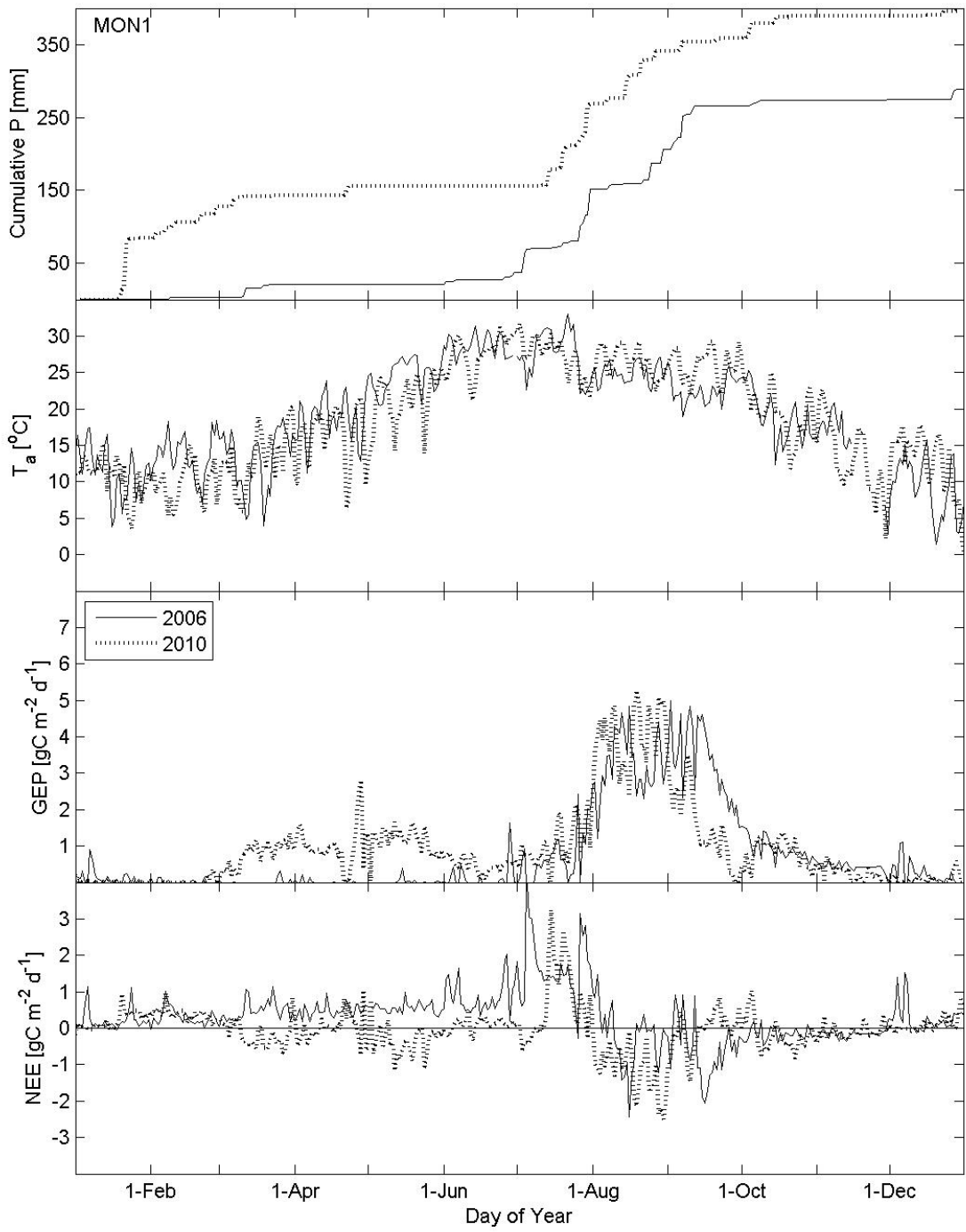
556
557
558

1
2
3
4
5
6
7
8
9
10
11
12
13
14
15
16
17
18
19
20
21
22
23
24
25
26
27
28
29
30
31
32
33
34
35
36
37
38
39
40
41
42
43
44
45
46
47
48
49
50
51
52
53
54
55
56
57
58
59
60
61
62
63
64
65



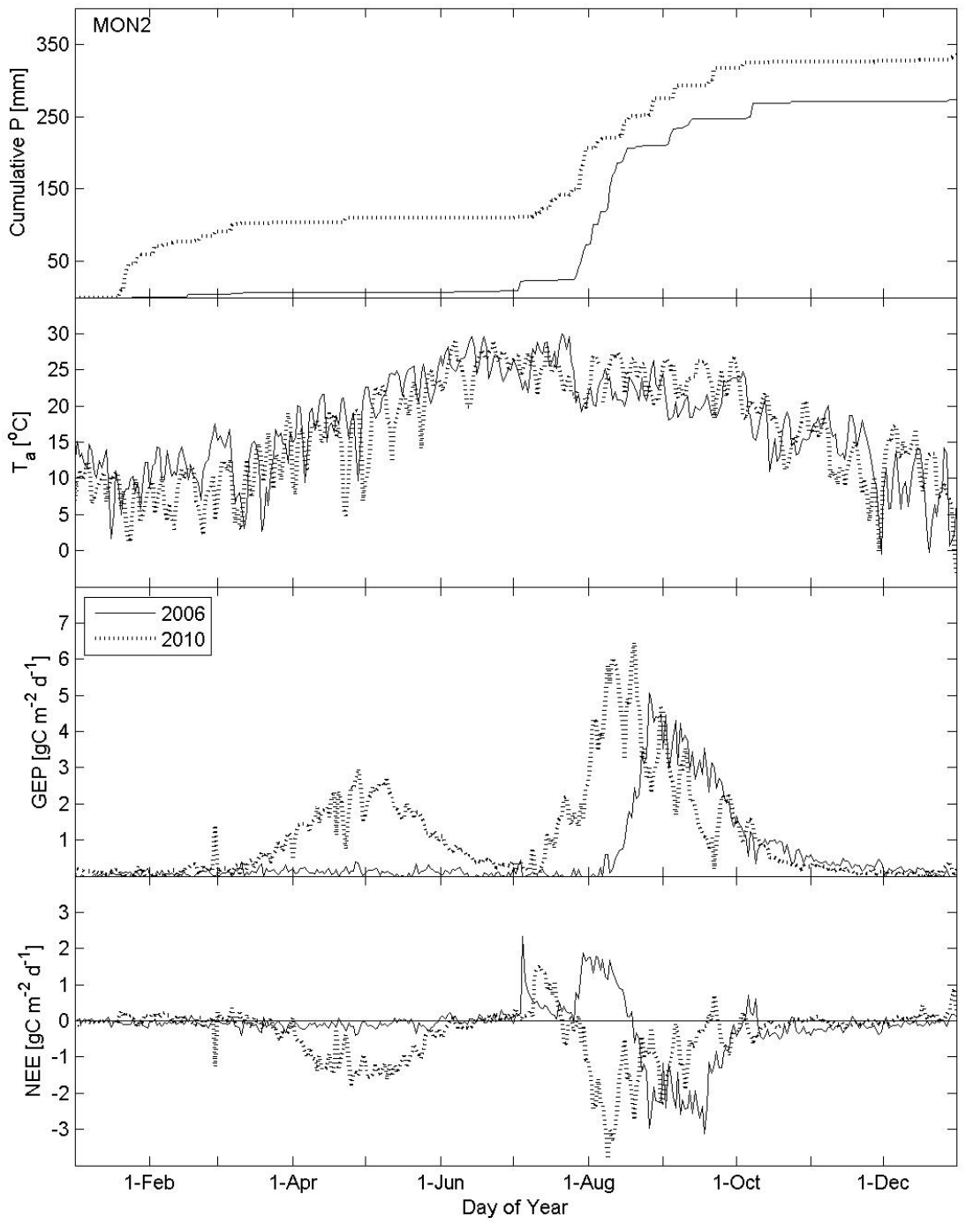
559
560

1
2
3
4
5
6
7
8
9
10
11
12
13
14
15
16
17
18
19
20
21
22
23
24
25
26
27
28
29
30
31
32
33
34
35
36
37
38
39
40
41
42
43
44
45
46
47
48
49
50
51
52
53
54
55
56
57
58
59
60
61
62
63
64
65



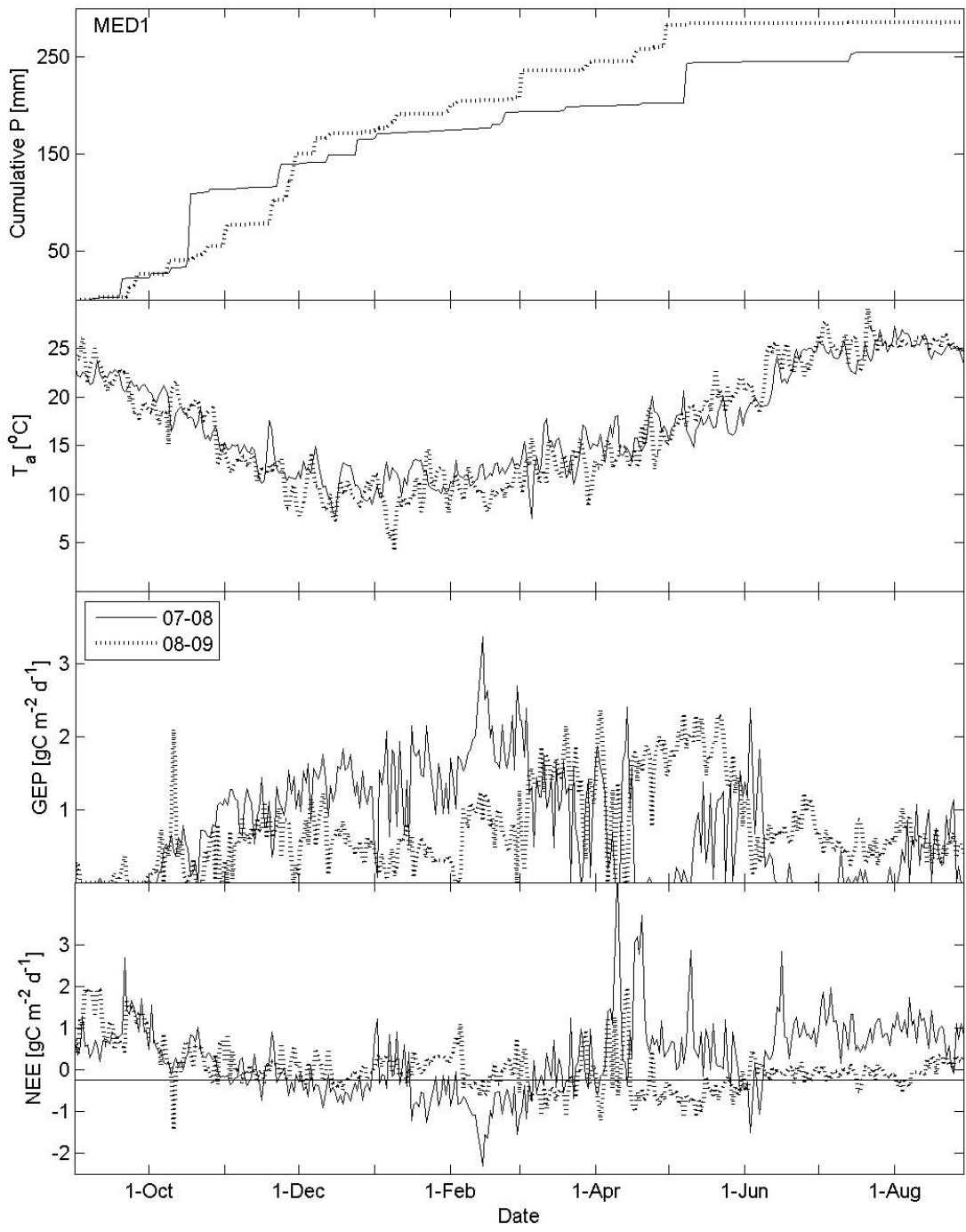
561

1
2
3
4
5
6
7
8
9
10
11
12
13
14
15
16
17
18
19
20
21
22
23
24
25
26
27
28
29
30
31
32
33
34
35
36
37
38
39
40
41
42
43
44
45
46
47
48
49
50
51
52
53
54
55
56
57
58
59
60
61
62
63
64
65



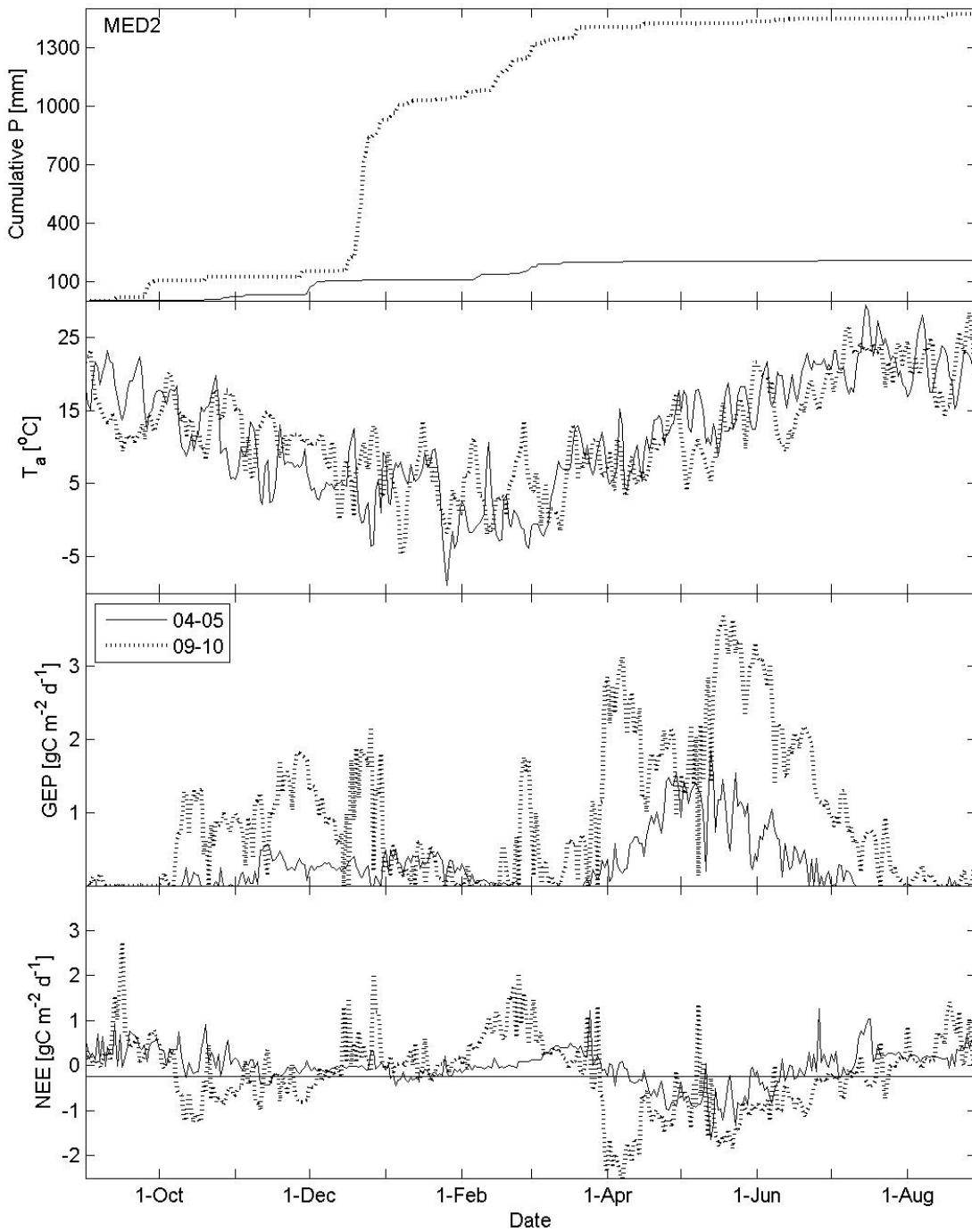
562
563

1
2
3
4
5
6
7
8
9
10
11
12
13
14
15
16
17
18
19
20
21
22
23
24
25
26
27
28
29
30
31
32
33
34
35
36
37
38
39
40
41
42
43
44
45
46
47
48
49
50
51
52
53
54
55
56
57
58
59
60
61
62
63
64
65



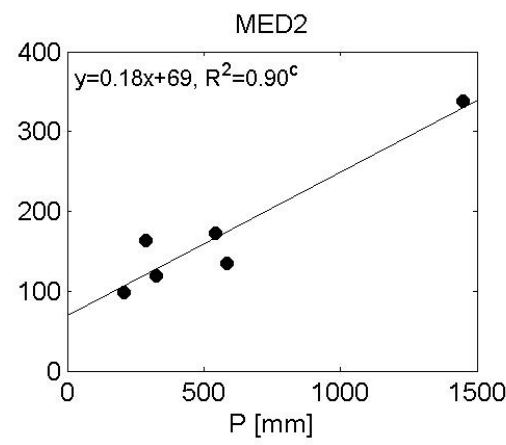
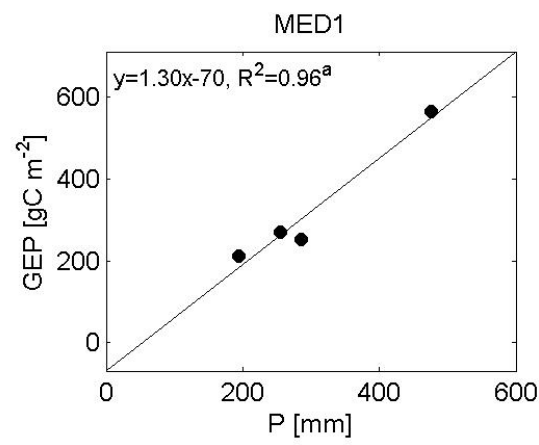
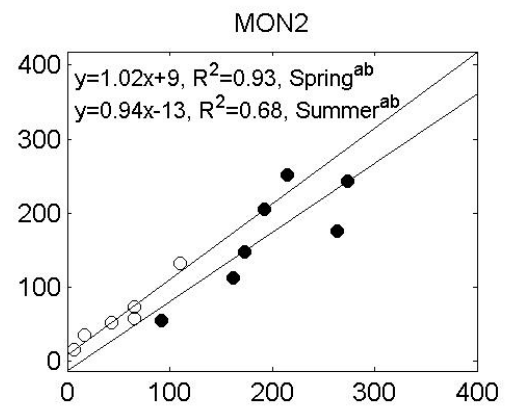
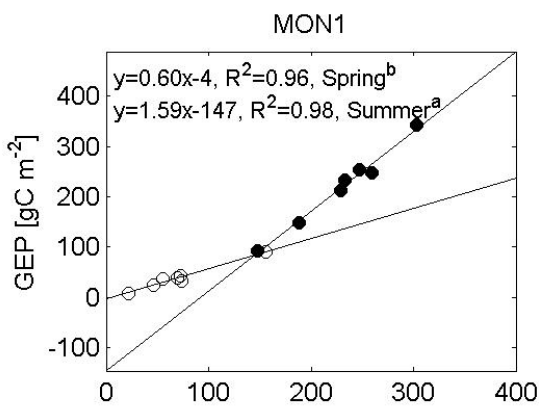
564

1
2
3
4
5
6
7
8
9
10
11
12
13
14
15
16
17
18
19
20
21
22
23
24
25
26
27
28
29
30
31
32
33
34
35
36
37
38
39
40
41
42
43
44
45
46
47
48
49
50
51
52
53
54
55
56
57
58
59
60
61
62
63
64
65



565
566

1
2
3
4
5
6
7
8
9
10
11
12
13
14
15
16
17
18
19
20
21
22
23
24
25
26
27
28
29
30
31
32
33
34
35
36
37
38
39
40
41
42
43
44
45
46
47
48
49
50
51
52
53
54
55
56
57
58
59
60
61
62
63
64
65



567

568

*Highlights

- > We compare carbon dioxide fluxes at semiarid Mediterranean and monsoon sites.
- > Fluxes at all sites showed periods of water and temperature/energy limitation for ecosystem photosynthesis and net carbon flux.
- > Precipitation magnitude and timing were the dominant drivers of ecosystem net carbon uptake and photosynthesis.
- > Low winter temperatures and/or light also regulated carbon exchange
- > Total photosynthesis was strongly linked to seasonal precipitation amounts at all sites, with some site and season level differences likely due to how rainfall is converted to available plant soil water.